Characterization and Evaluation of Controls on Post-Fire Streamflow Response Across Western U.S. Watersheds

Samuel Saxe[1], Terri S. Hogue[1], and Lauren Hay[2]

[1]Civil and Environmental Engineering and Hydrologic Science and Engineering, Colorado School of Mines, Golden, Colorado, USA
[2]National Research Program, United States Geological Survey, Lakewood, Colorado, USA

Correspondence to: Samuel Saxe (ssaxe@usgs.gov)

Abstract. This research investigates the impact of wildfires on watershed flow regimes, specifically focusing on evaluation of fire events within specified hydroclimatic regions in the western United States, and evaluating the impact of climate and geophysical variables on post-fire streamflow response. Eighty two watersheds were identified with continuous pre- and post-fire daily streamflow records. Percent change in annual runoff ratio, low-flows, high-flows, peak flows, number of zero flow days, baseflow index, and Richards-Baker flashiness index were calculated for each watershed using the pre- and post-fire periods. Independent variables were identified for each watershed and fire event, including topographic, vegetation, climate, burn severity, and soils data. Watersheds were divided into nine regions through k-means clustering according to climate variables.

Results show that low flows, high flows, and peak flows increase significantly in the 1st two years following a wildfire and decrease over time. Relative response was utilized to scale response variables with respective percent area of watershed burned in order to compare regional differences in watershed response. Watersheds in eastern California, western Nevada, and Oregon demonstrate a slight negative response in the post-fire observed flow regimes. Watersheds in coastal California display the greatest change in flow response, typically within the 1st post-fire year. Most other watersheds show a positive mean relative response. The regression models show limited correlation between percent watershed burned and streamflow response, implying that other watershed factors strongly influence response.

Post-fire changes in streamflow are found to be highly variable across regions of the western U.S. and some trends can be difficult to discern. Spearman correlation, regression models, and random forest models were applied in an attempt to identify the influence of watershed parameters on streamflow response but produced conflicting results. Typically, factors such as burn severity, slope, and watershed area were found to be the most important geophysical properties of a burned watershed.

Results from this study will help inform post-fire runoff management decisions as well as facilitate parameterization for model application in burned watersheds.

1 Introduction

The number of wildfires in the western United States (US) is increasing annually, on average costing federal agencies billions of dollars a year in suppression efforts (Whitlock, 2004) and causing an increase in flood events destructive to both life and infrastructure (Neary et al., 2005; Pausas, 2008). Westerling et. al. (2006) showed that the western fire regime exhibited a significant transition from infrequent and short-duration events to higher frequency, longer duration regimes during the mid-1980's. The greatest increases in fire frequency were found to occur in mid-elevation forests, most commonly in the Northern Rockies, Sierra Nevada, southern Cascades, and western Coast Ranges in northern California and southern Oregon (Littell et al., 2009). This marked change is strongly correlated with climate change impacts, such as warmer springs and longer dry seasons, commonly in occurrence with reduced winter precipitation rates and earlier spring snowmelt. Overall, Westerling et. al. 2006 determine that, though land-use history may be a significant factor in the spatial distribution of wildfires within specific forest types, changes in fire regimes in the western US are most likely be attributable to recent changes in climate. Other notable research has also provided significant correlatory evidence between climate change and wildfire occurrences (Littell et al., 2009; Moritz et al., 2010).

Though wildfires are a part of the natural process of vegetation dynamics, they cause wide-ranging changes to ecosystems (Daniel G Neary, 2003; Santos et al., 2015) depending on numerous factors, most importantly burn severity. Studies examining the effects of wildfires on a small-scale, such as in plot-sized and laboratory experiments, show high fire temperatures can result in the combustion of organic matter within soils and cause permanent alteration to the chemical structure of local clays, decreasing soil stability (Shakesby and Doerr, 2006). Water-repellent soil layers can be created in a discrete layer on or below the soil surface through chemical bonding of the combusted organic matter to mineral particles, potentially increasing overall topsoil erosion rates in burned regions (Wilkinson et al., 2009), though this hydrophobicity is highly variable depending on fire behavior, burn severity and soil properties (DeBano, 2000).

At larger scales, such as entire watersheds or multiple watershed systems, studies of post-fire erosion rates have shown incompatible conclusions (Moody and Martin, 2001; Owens et al., 2013; Smith et al., 2011), though this is most likely due to the variability of precipitation events and general climate patterns (Moody et al., 2013). In terms of water quality, contaminant levels can be dramatically increased for many years after a wildfire in both soil (Burke et al., 2010) and stream systems (Emelko et al., 2011; Stein et al., 2012; Burke et al. 2013), increasing the workload on source water protection organizations in communities reliant upon burned watersheds for drinking and farm water. Furthermore, wildfires are readily attributed as the cause of substantial increases in debris flows (Benavides-Solorio and MacDonald, 2001; Cannon et al., 2001; Meyer et al., 2001).

Studies evaluating post-fire water yield change are highly disparate owing to the transient nature of climate patterns, variations in basin geomorphology, and vegetation recovery patterns, and the resulting complex interactions (Moody et al., 2013). For example, studies in rangeland regions of the US found moderate increases in flow, infiltration, and erosion rates after major wildfires, with trends continuing for as long as 15 years (Emmerich and Cox, 1994; Pierson et al., 2009; Hester et al., 1997; Kinoshita and Hogue, 2015). Fires in chaparral environments, such as in southern California, exhibited increased flows up to

as much as two orders of magnitude, with much of this occurring in the dry season (Coombs and Melack, 2013; Kinoshita and Hogue, 2011 and 2015; Loáiciga et al., 2001). Fires in other chaparral environments were found to also yield flow increases, such as in South Africa (Lindley et al., 1988; Scott, 1993), Cyprus (Hessling, 1999), and France (Lavabre et al., 1993). Additional increases to post-fire flow regimes were found in temperate, forested catchments as well (Neary et al., 2005; Watson et al., 2001). A concise summary of historic changes in US post-fire stream systems is found in Neary et al. (2005), documenting changes in 1st year runoff and peak flows, encompassing a range of ecological regions. Conversely, several studies found limited or no significant changes to hydrologic systems post fire, or attributed fluctuations to natural annual variability (Aronica et al., 2002; Bart and Hope, 2010; Britton, 1991; Townsend and Douglas, 2000).

These discrepancies in post-fire flow response lead to the question of which watershed characteristics have the greatest influence over the observed response? Moody et al. (2013) provide a succinct summary of soil-related theories, such as reduced infiltration due to increases in soil-water repellency, increased overland flow velocities due to increased bare ground, and reduced infiltration caused by soil-sealing. Theories commonly found in literature attribute flow changes to a wider range of factors, including reduction in interception and evapotranspiration (Lavabre et al., 1993; Scott, 1993) and increased hydrophobicity of soils (Neary et al., 2005). In regards to altered peak flows, conflicting evidence is found regarding the importance of burned watershed areas with some studies finding an inverse correlation between peak flows and watershed size (Biggio and Cannon, 2001; Neary et al., 2005) and others finding no relation at all (Bart and Hope, 2010).

The current research builds upon prior studies but develops a more comprehensive and systematic assessment of post-fire streamflow dynamics by examining burned watersheds that encompass a wide spectrum of climatological and geophysical parameters across the western US. A variety of statistical parameters are also examined which describe changes to flow regimes at several levels. Furthermore, the variability in response by distinct regions is investigated, anticipating distinct differences influenced by regional climate. With downstream communities at risk for flooding, and also relying on catchment runoff for water supply, investigating alterations in post-fire discharge over large scales will provide critical information for regional managers on post-fire runoff mitigation. In addition, understanding factors controlling discharge response will help inform development and calibration of surface water models used for post-fire streamflow predictions.

2 Study Area

A total of 82 burned watersheds were utilized (Fig. 1), encompassing a range of spatial, temporal, climatological, and topographic factors (Fig. 2). Selected watersheds were limited to those with burn areas of > 5% and adequate discharge records (continuous 15 years daily flow) (U.S. Geological Survey, 2014) identified through the GAGES-II database (Falcone, 2011). The majority of available watersheds are overwhelmingly found in the western US, predominantly in California, Oregon, and Idaho. Due to discharge and burn severity data limitations, the fires cover a temporal range from water years 1984 through 2010. Percent area burned ranges from 5-97%, with a mean of 25%, over a range of watershed areas from 4.6-9209 km2. The wide spatial distribution of the studied watersheds results in mean elevations and burn-area slopes varying from 13-2760 m and 0.11-16% respectively (Fig. 2).

The most important difference between many of these watersheds is the variability in climate, the values of which were collected from the GAGES-II dataset (Falcone, 2011). GAGES-II watersheds have at least one twenty year period with continuous daily flow records. Average basin precipitation ranges from 29-220 mm/yr, with a mean of 72 mm/yr, and average temperature ranges from 1.4 -23 °C, with a mean of 10 °C. Important for identifying snow dominated regions is the percent of precipitation (PPT) that falls as snow (%Snow/PPT), which ranges from 0-72% for the study watershed. Relative humidity ranges from 39-73%, with a mean of 55, and potential evapotranspiration ranges from 400-1200 mm/yr, with a mean of 633 mm/yr.

Vegetation types vary across the watersheds as well. Evergreen forest and shrub vegetation are the dominant land cover type over all watersheds used in this study (Fig. 3). The high proportion of evergreen is due to the dominance of high elevation fires in mountainous regions and shrub prevalence is due to the abundance of watersheds found in the chaparral regions of Southern California. Grassland, mixed forest, and developed land account for a smaller proportion of land cover types. Barren land and wetland account for only a small percentage of land cover types throughout the watersheds in this study.

3   Methods

3.1   Data Collection

Watershed parameters were chosen to encompass the variability in geophysical and climatic conditions found throughout the watersheds used in this study (Table 2.1). To identify spatial trends in post-fire response, watersheds were 1st grouped through k-means clustering based on geographic and climatological data (described in section 3.1 below).
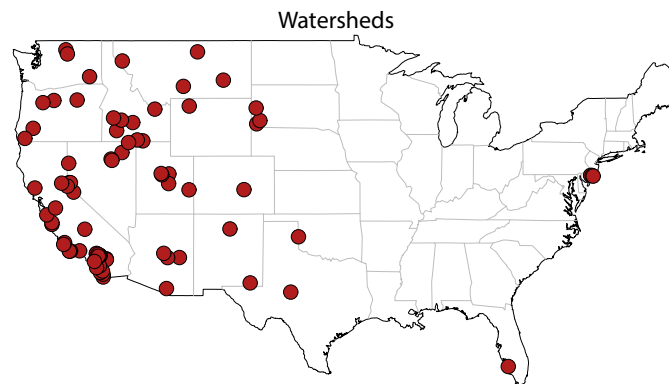
Figure 1. CONUS scale map of the locations of the 82 watersheds utilized in this study.
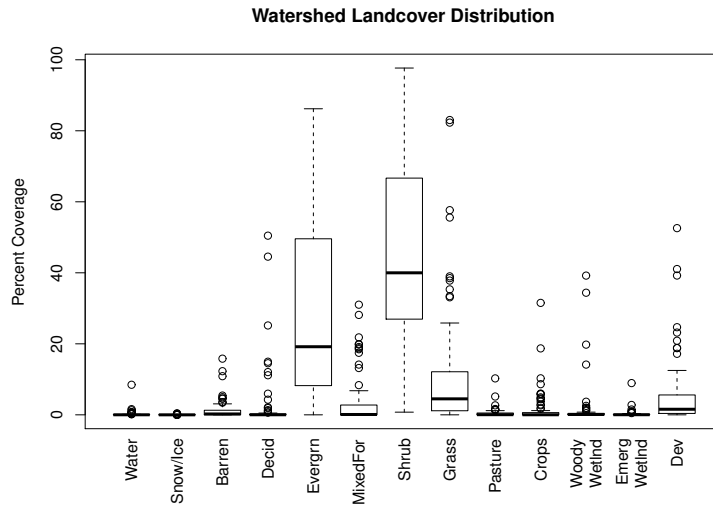
Figure 2. Boxplot of National Land Cover Database distribution across study watersheds.
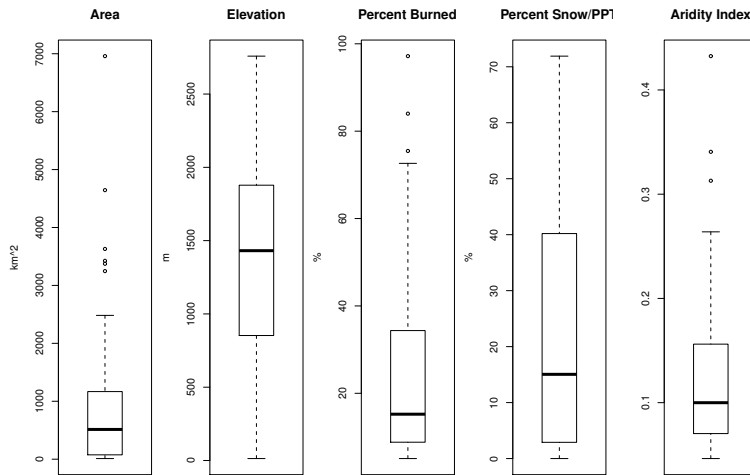
Figure 3. Boxplots summarizing the distribution of watershed area, elevation, percent area burned, precipitation that falls as snow, and airidity index across study watersheds.

3.1.1 Watershed Selection

Selected watersheds were required to have continuous daily flow records (more than 95% of daily flow records accounted for in each year) for a minimum of 10 years pre-fire and 5 years post-fire. Using the approximately 9,000 watersheds in the

GAGES-II dataset (Falcone, 2011), delineated watersheds were spatially cross-referenced with the MTBS database of historic wildfires (Eidenshink et al. 2007). The results were again cross-referenced with USGS daily flow records (U.S. Geological Survey, 2014) to identify watersheds with the required flow records, resulting in 263 unique watersheds in the US with greater than 5% total burn area in a single water year. Of these, 23 contained 2-3 wildfires within the same year burning over 5% of the total area. The remainder contained only a single significant fire in the year of interest. Further exclusion of watersheds was based on the presence of major dams within the watershed flow regimes extracted from the GAGES-II database (Falcone, 2011), resulting in a final collection of 82 watersheds.

3.1.2   Streamflow and Precipitation Data

Daily flow and peak flow data were obtained from the USGS National Water Information System (U.S. Geological Survey, 2014), matched for the range of 10 years pre-fire and 5 years post-fire for each selected watershed. Monthly precipitation data was collected from the PRISM database, a nation-wide 4 km resolution gridded monthly dataset that extrapolates station climate measurements over unmonitored areas using a topographic- and climate-based algorithm (PRISM Climate Group, 2004). Monthly national precipitation rasters were averaged for each watershed for all months within the flow record period.

3.1.3   Climatological data

Watershed climatological parameters included percent of precipitation that falls as snow (%Snow/PPT) and the aridity index (AI). The %Snow/PPT for each watershed was available through the GAGES-II dataset (Falcone, 2011) and the aridity index was calculated for each watershed as:

$$AI = \frac{P_{avg}}{PET_{avg}} \tag{1}$$

where P_{avg} is average precipitation and PET_{avg} is average potential evapotranspiration, both of which were available in the GAGES-II dataset.

3.1.4   Burn Severity data

Burn severity is the classification of burn areas relating visible changes in living and non-living biomass, fire byproducts, and soil exposure within one growing season, including low, moderate, and high severity categories (Eidenshink et al., 2007). Though categorization varies by region, some generalizations can be made. Typical high severity burns result in complete kills of canopy trees and almost complete consumption of surface litter and organic soil layers (Neary et al., 2005). Characteristics of moderate burn severity include partial canopy cover kill, completely charred or consumed understory vegetation, and widespread destruction of the soil organic layer. Low severity burns lightly scorch trees, char or consume surface litter, and produce little to no charring of the soil organic layer. Wildfires are almost always a patchwork of varying degrees of burn severity. More specifically, burn severity is the qualitative assessment of the heat pulse directed toward the ground during a fire, relating soil heating, fuel consumption, and mortality of buried plant parts (National Wildfire Coordinating Group, 2016). Burn severity data were obtained for each unique fire through the MTBS database (Eidenshink et al., 2007) and quantified as

the percent area burned of the total watershed area. Values were categorized as unburned-low severity, moderate severity, and high severity.

3.1.5 Vegetation data

Vegetation data were collected for each burn area prior to the fire event. Due to the temporal gaps in the National Land Cover Database (Homer et al., 2004), an averaged normalized difference vegetation index (NDVI) was collected for pre-fire burn areas to quantitatively summarize vegetation conditions, similar to previous studies (Barbosa et al., 1999; Kinoshita and Hogue, 2011; Lee and Chow, 2015). NDVI is defined as:

$$NDVI = \frac{a_{nir} - a_{vis}}{a_{nir} + a_{vis}} \tag{2}$$

where a_{nir} and a_{vis} are surface reflectance averaged over the ranges of wavelengths in the near infrared and visible spectrums, respectively. Despite NDVI having been shown to have accuracy issues related to atmospheric interference and variations in soil brightness (Carlson and Ripley, 1997), the extended timespan over which values were being averaged may have muted any such error responses.

Average values were collected for each watershed through national 32-day NDVI rasters hosted on Google Earth Engine (GEE) (Google, Inc.), in turn calculated from Landsat5 composite satellite data freely available through the U.S. Landsat archive at the USGS Earth Resources Observation and Science (EROS) Center (Woodcock et al., 2008). Mean NDVI values were produced for the burn areas of all watersheds for four years pre-fire.

3.1.6 Soils data

Soils data were collected through an adapted version of the State Soil Geographic (STATSGO) database, a national collection of over 78,000 polygons containing a host of soil characteristics (Schwartz and Alexander, 1995). The soil erodibility factor (Kfact) was utilized to numerically represent average soil types, as it provides a quantitative description of a soil's erodibility. The calculation included values of particle size, percent organic matter, percent clay, soil structure index, and profile-permeability class factor (Goldman et al., 1986). Kfact increases as the potential erodibility of a soil increases.

3.1.7 Topographic data

Collected topographic data included watershed area and the elevation, slope, and aspect of burn areas, calculated through a 30 meter resolution CONUS Digital Elevation Model. Percent burn areas of watersheds through intersection of watershed and MTBS fire polygons.

3.2 Response Variables

A range of response values were selected to quantify post-fire flow changes across a variety of regimes, including flows relating to dry season (low flows, base flows) and wet season (high flows, peaks flows).

3.2.1 Low, high, and peak flows

Low flow and high flow metrics were calculated for each of the ten water years prior to the fire and averaged to produce a single value. Low flows were defined as the average of mean daily flows with a 90% exceedance within a single water year. To reduce calculation bias due to zero flow days commonly found in ephemeral stream systems, zero flow days were eliminated from exceedance value calculations. High flows were defined similarly, with a 10% exceedance threshold used to isolate larger volume flows (Kinoshita and Hogue, 2015). Changes in low flows and high flows were calculated as the post-fire percent change from the average of 10 water years pre-fire. Post-fire values were calculated for the 1st year, the 2nd year, and the 5 year mean. Peak flows were defined as the largest mean daily flow measurement each water year and post-fire changes were calculated as the percent change of the 1st year, 2nd year, and 5 year mean peak flow measurements from the pre-fire ten year mean. Percent changes in the number of zero flow days were calculated similarly.

3.2.2 Runoff Ratios

The runoff ratio is defined as the fraction of total annual runoff depth over total annual precipitation:

$$RO = \frac{Q_{tot}/A_{ws}}{P_{tot}} \tag{3}$$

where P_{tot} is total annual precipitation, Q_{tot} is total annual runoff depth, and A_{ws} is watershed area. Runoff ratio was calculated for the ten years pre-fire and 5 years post-fire using PRISM precipitation and USGS mean daily flow data. Post-fire runoff ratio response was calculated as the percent change between the 1st year, 2nd year, and average 5 year values post-fire and the pre-fire 10 year mean.

3.2.3 Base flow and Richards-Baker indices

Base flow index, defined as the fraction of total streamflow that is baseflow (Baker et al., 2004), was calculated for each water year through the R package 'hydrostats' (Bond, N., 2015), that applies the Lyne-Hollick filter (Ladson et al., 2013). Baseflow index response was calculated as the percent change of the 1st, 2nd, and 5 years post-fire from the mean of the 10 years pre-fire.

The Richards-Baker index quantifies the frequency and rapidity of short-term changes in streamflow (flashiness) based on daily flow data through the equation:

$$R - BIndex = \frac{\sum_{i=1}^{n} |q_i - q_{i-1}|}{\sum_{i=1}^{n} q_i} \tag{4}$$

where q is mean daily flow, t is time, and q is daily flow (Baker et al., 2004). Richards-Baker response was calculated as the percent change from the average value over the ten years pre-fire to the average 1 year, 2 years, and 5 years post-fire.

3.3 k-means Clustering

To create region-specific regression models, watersheds were classified into unique areas through k-means clustering (MacQueen, 1967) based on all GAGES II watersheds. This approach partitions an N-dimensional population of observations into
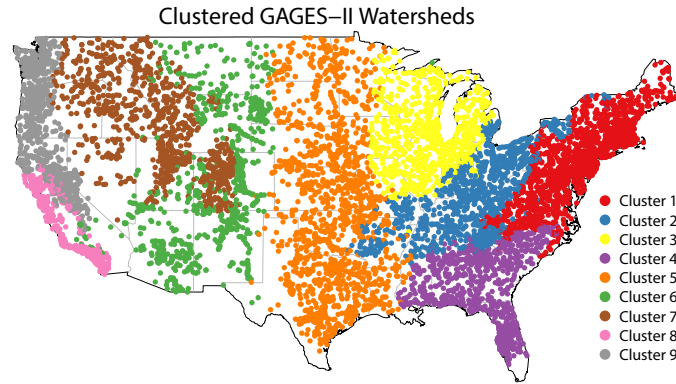
Figure 4. CONUS scale map of the results of k-means clustering of the GAGES-II watershed set by climate variables.
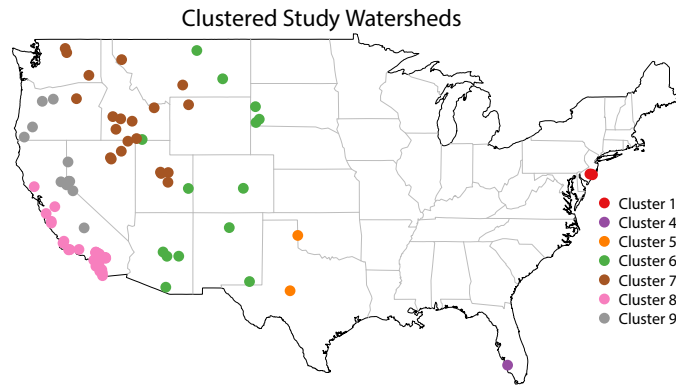
Figure 5. CONUS scale map of the k-means clustered study watersheds.

clusters with minimal variation, allowing for relatively simple similarity grouping. For the current study, the ideal ensemble of clusters was one that produced easily recognizable regions with unique climatological characteristics. Large-scale clustering methods have been applied in prior watershed classification studies, but utilized more complex streamflow and ecological indices as parameters (McManamay et al., 2014; Poff, 1996).

5   Wildfires in this study are primarily in western evergreen and shrub environments, so clustering using only these watersheds would likely produce regions biased by fire occurrence. To limit this impact, we applied the mclust package in R (Fraley et al., 2012) to cluster using the entire 9,000 GAGES-II watersheds to produce national regions. The mclust package was chosen over the standard kmeans function in R due to its inclusion of numerous model-based approaches and application of the Bayes Information Critera (BIC) to determine the most accurate model and cluster count (Schwarz, 1978). Various groupings of

10   simple parameters were used for clustering including watershed latitude and longitude, elevation, AI, %Snow/PPT, and mean monthly and seasonal flow statistics.

3.4 Control Evaluation Methods

Characterization of the influence of watershed geophysical parameters on flow response was performed using three approaches. 1st, calculation of the Spearman correlation coefficient between independent and response variables. 2nd, calculation of two types of regression equations: 1) a standard multiple linear regression model, and 2) a logistic regression model where responses greater than 20% are assigned a value of 1 and responses less than 20% are assigned a value of 0. Third, application of a conditional inference tree algorithm through the "party" package in R (Hothorn et al., 2006). This algorithm 1st applies a significance test to identify the independent variables that have the strongest association with the response variable. It then searches for the best split points in those independent variables to partition the data into a tree.
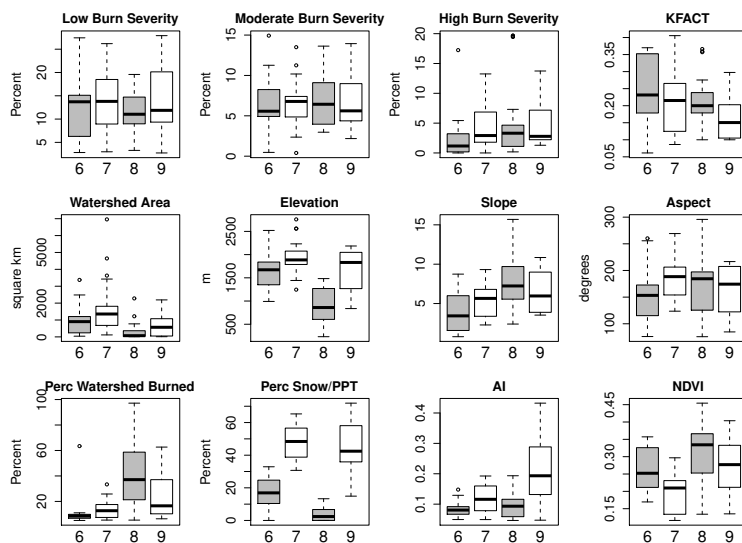
Figure 6. Boxplots of the variation in explanatory variables by cluster.

4 Results and Discussion

4.1 Clustering

The k-means clustering performed on the GAGES-II watershed set yielded 9 clusters or regions (Fig. 4). The most important clusters for the current study are 6 through 9, which assemble 77 of the 82 watersheds into unique regions (Fig. 5). These four clusters have unique characteristics (Fig. 6). Watersheds in cluster 6, on average, have the highest Kfact, though almost all are burned less than 20%. They have relatively moderate %Snow/PPT values and the lowest AI values. Watersheds in cluster 7 have the highest average area and elevation, and accordingly the highest %Snow/PPT and the lowest NDVI. Cluster 8 contains watersheds with the widest range of relative fire sizes, including watersheds burned from as little as 10% to as great as 97%. Watersheds in cluster 8 also have the lowest average elevations and areas, as well as the smallest %Snow/PPT and low AI. The

percent of the burn area rated as high burn severity is also the greatest, on average, in cluster 8 watersheds. Cluster 9 watersheds have the lowest KFACT and highest elevations. These watersheds also have high %Snow/PPT and AI.

4.2   Response Variable Distribution and Analyses

Calculated flow response variables indicate an extremely wide range of post-fire system responses (Fig. 7). The greatest ranges occur within variables representing changes in low flows, such as 1st year change to number of zero flow days (st. dev = 243%), 1st year baseflow index (236%) and five year change to number of zero flow days (201%). The tightest ranges are typically found within mean five year variables where extreme changes are muted, such as five year Richards-Baker (28%), runoff ratio (39%), and baseflow index (48%). Response variable means range from as low as 0.92% (five year Richards-Baker) to as great as 115% (1st year change to number of zero flow days). Due to the nature of response calculations, number of zero flow day values were limited. 1st and 2nd year zero flow day responses were found for only 22 watersheds, and for 27 watersheds for the five year values.
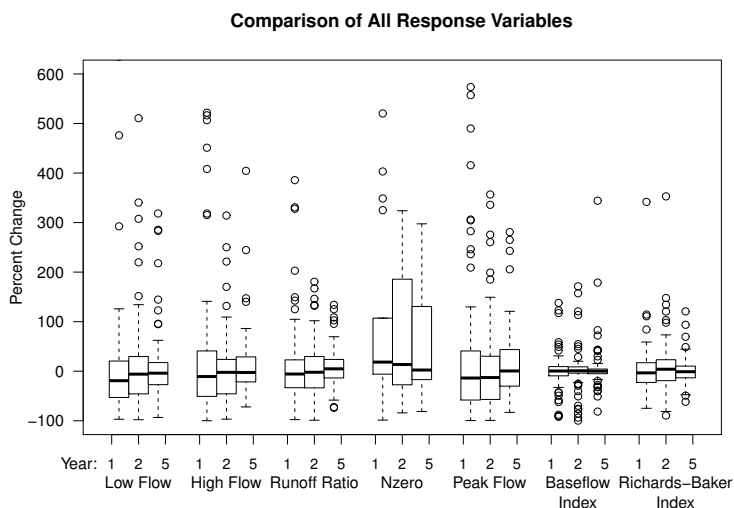
Figure 7. Boxplot of the distribution of response variables utilized in this study. Nzero refers to number of zero flow days.

4.2.1   Trend Analysis

Comparison of 1st year response variables to 5 year mean variables typically results in slope values greater than one, with a mean slope of 1.9 (Fig. 8) and the greatest slopes being found in 1st year low flow, high flow, and baseflow index response variables. Best fit lines of 2nd year response variables versus 5 year mean variables produce significantly lower slopes, with a mean of 0.78. We can infer from this that the greatest increases in these response variables are typically generated in the 1st year following a fire. Similarly, in comparing response variables to percent area burned (Fig. 9), best fit lines show the
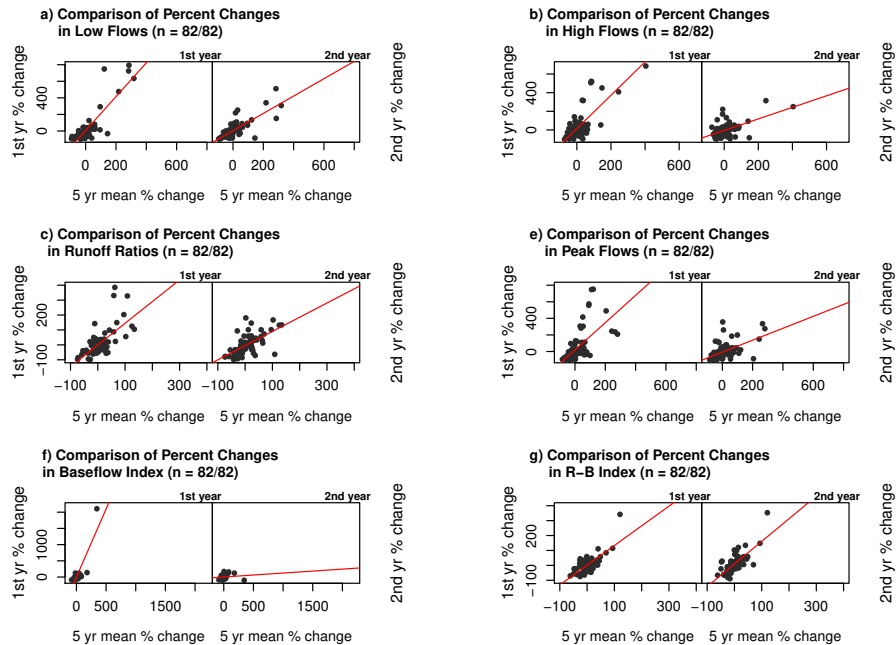
Figure 8. Scatterplots of 1st and 2nd year response variables versus 5 year means with lines-of-best-fit.

greatest slopes in 1st year values for low flows, high flows, and peak flows. Slopes in 2nd year values are almost always less than those of the 1st year values and almost always greater than those of the 5 year mean values. The exception to this are 2nd year number of zero flow days values that decrease with increased fire size. Overall, number of zero flow days is observed to increase post-fire, though due to both a small sample size and a short time period, results are most likely unreliable. Only Richards-Baker indicates little linear correlation to burn area, yielding marginal 1st and 2nd year slopes, and five year mean values decrease with percent area burned. These findings largely confirm those of previous studies which posit that the largest changes in streamflow are typically found in the 1st year after a wildfire. While there is significant noise in the data, we find similar results. While response tends to increase overall within five years of a wildfire, the greatest increases are frequently found within the 1st year.

4.2.2 Response variability by cluster

Boxplots for response variables show differences across the four significant clusters noted above (Fig. 10). In this instance and that of the CONUS plots, all variables are scaled by dividing the variable by the percent burn area of the watershed in order to show relative response. Generalizing variability and magnitudes, dramatic differences can be established between clusters. Most noteworthy is Cluster 9, which dominantly produces negative streamflow responses post-fire. The largest magnitude relative responses are found in Cluster 6, which results in the greatest variability between variables (st.dev = 8.5). The most positive responses are found in Cluster 8, which frequently exhibits large positive responses and infrequent low negative
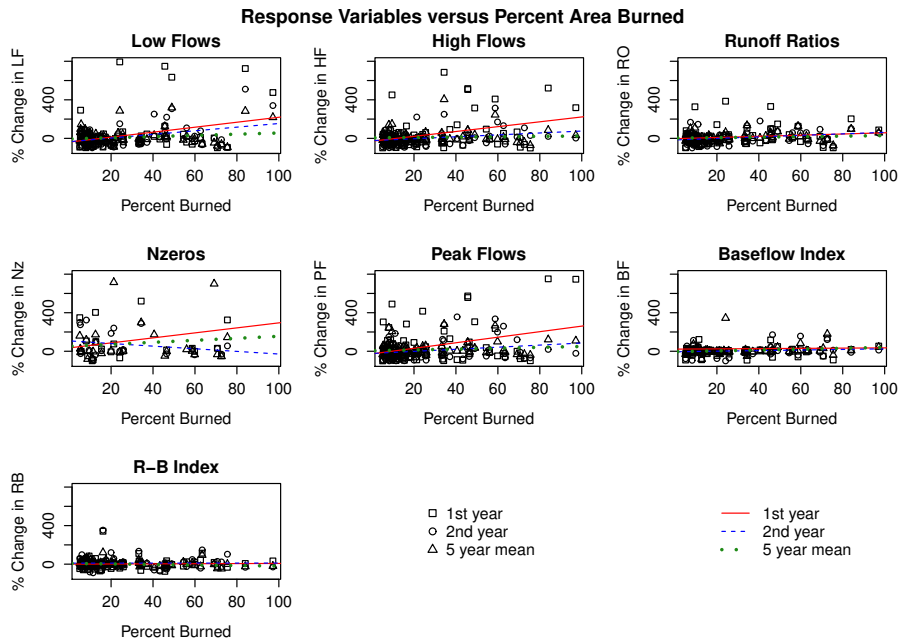
Figure 9. Scatterplots of response variables versus percent watershed burned. Best fit lines provided to demonstrate correlation.

responses. Cluster 7 produces low magnitude responses. Though they are, on average, positive there are also several negative responses.

Evaluating cluster responses when they are not scaled relative to fire size shows many similarities to the transformed results. For instance, average response in Cluster 9 is still dominantly negative with an overall low magnitude. Cluster 8 demonstrates

5   the greatest overall variability and magnitude. On average, response in this cluster is strongly positive. Cluster 7 responses are small relative to other clusters in this study with a negative trend. Cluster 6 still exhibits high variability and low magnitude. What we surmise from these results is that watersheds in the Cluster 8 region will most likely be impacted the most from wildfire in terms of flow response. Watersheds in Clusters 7 and 9 see substantially lower responses, if any at all. Cluster 6 may prove to be the most difficult to predict due to its high variability in response.

10   Evidence of temporal patterns is sometimes noticeable when examining response by cluster. In Clusters 6 and 9, there are no distinct trends between 1st, 2nd, and five year mean relative values. In some response variables, there are increases in the actual values of 2nd year variables within Cluster 9. Cluster 7 typically shows negative relative and actual responses in 1st year values, but increasing positive values in the 2nd and five year means. Cluster 8 produces largest response values in the 1st year after a fire. Relative values tend to be negative in the 2nd year and positive over the five year mean. Actual values are still

15   positive in the 2nd year.

By examining response values by cluster, we are able to identify more intricate and robust trends than by simply examining the dataset as a whole. Spatially, we find that watersheds in Cluster 8 produces much greater and more predictable post-fire
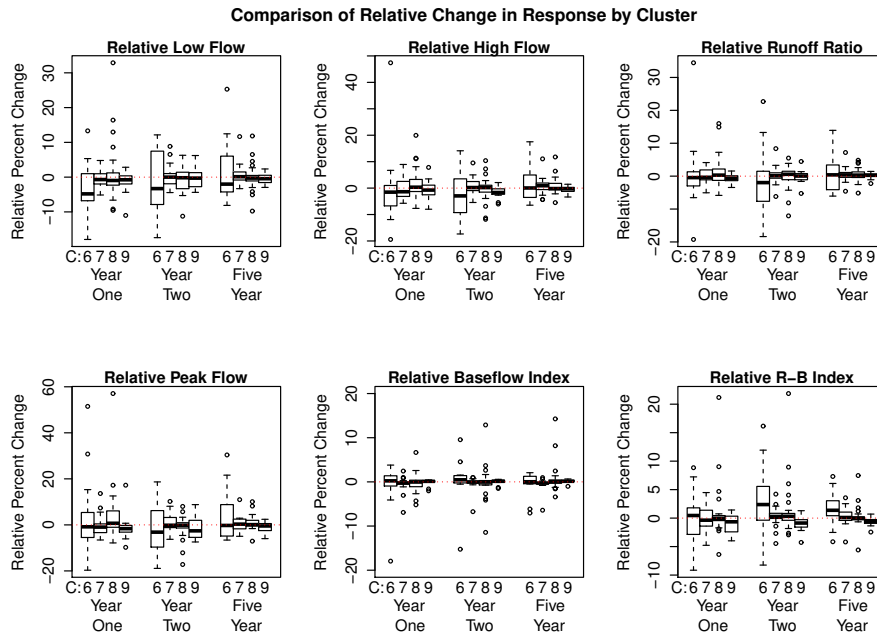
Figure 10. Boxplots of relative response variables by cluster. Relative response is actual response divided by percent area burned, in order to show response relative to fire size.

flow responses than watersheds in Cluster 6, 7, and 9. Responses in Clusters 7 and 9, overall, tend to be low magnitude and negative. Cluster 6 watersheds yield highly variable responses. Temporally, watersheds in Cluster 8 follow the trend found when examining all study watersheds as a whole, with greatest responses occurring in the 1st post-fire year and decreasing over time. However, the magnitude of the response of these fires skewed the results of the generalized examination at the

5   beginning of this section. Cluster 7 watersheds, in fact, produce decreased responses in the 1st year post-fire with increased flows occurring at the 2nd year and five year mean time periods. Clusters 6 and 9 exhibit little to no temporal trends at all.

    Variability in response variables also generally decreases with increasing percent watershed burned. Linear regression modeling of response variables by percent watershed burned yields the error statistics found in Figure 10 (i.e. decreasing sample size with increasing percent area burned). Figures include the adjusted R^2 and p-value significance tests (alpha = 0.05). Gener-

10   ally, linear modeling of 1st year response variables increases in accuracy as included values are limited by increasing percent burn area. 1st year low flow, high flow, peak flow, and Richards-Baker variables show substantial increases in adjusted R^2 once included watersheds are limited to those exceeding a 50% burn area (n=12). Included p-values indicate that several of the 1st year low flow and peak flow models are statistically significant.

    Applying the same methods to 2nd year values shows dissimilar results, with adjusted R^2 exceeding 0.5 in only a single

15   instance (2nd year high flows), and few significant p-values. However, in the cases of 2nd year low flow and Richards-Baker, R^2 values increase with increasing percent burn threshold. Unsurprisingly, simple regression of 5 year mean values versus percent
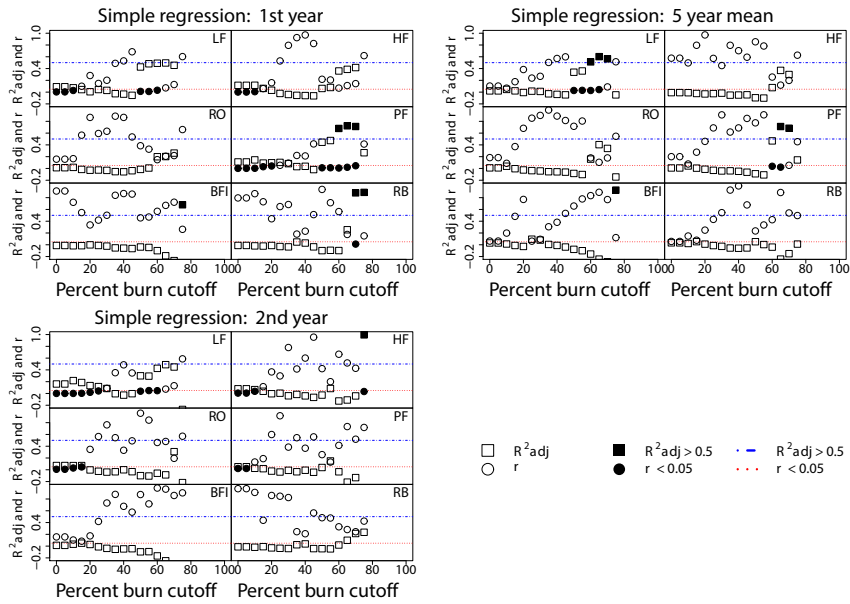
Figure 11. Scatterplots of the R^2 and p-value results of simple linear regression modeling of response variables versus an increasing percent burn limitation. Response variables are abbreviated as LF (low flow), HF (high flow), RO (runoff ratio), PF (peak flow), BFI (base flow index), and RB (Richards-Baker).

area burned produce mixed results with only 5 year mean low flow and peak flow allowing for adjusted R^2 values greater than 0.5, few of which are statistically significant. 5 year mean baseflow index shows a single instance of a high adjusted R^2 value but is statistically insignificant. Simple regression modeling was also performed on response variables by limiting included watersheds by decreasing percent area burned (i.e. decreasing sample size with decreasing percent area burned) and results

5   demonstrated zero significant adjusted R^2 values.

4.3   Influence of Geophysical parameters on response

4.3.1   Spearman Correlation

Spearman correlation between the independent and dependent variables, averaged across response variables, shows somewhat muddled results (Fig. 12). Generally, NDVI, AI, %Snow/PPT, and slope are positively correlated with flow response. Low burn

10   severity, KFACT, and watershed area are typically negatively correlated with flow response. Thus, as NDVI, AI, %Snow/PPT, and slope increase, response increases. As low burn severity, KFACT, and watershed area increase, response decreases. More difficult to interpret are the results for other independent variables, including moderate burn severity, high burn severity, elevation, etc. The correlation of these variables appears to switch from positive to negative by cluster. Ascertaining a significance for their relationships may be impossible via correlation for such a small sample size.
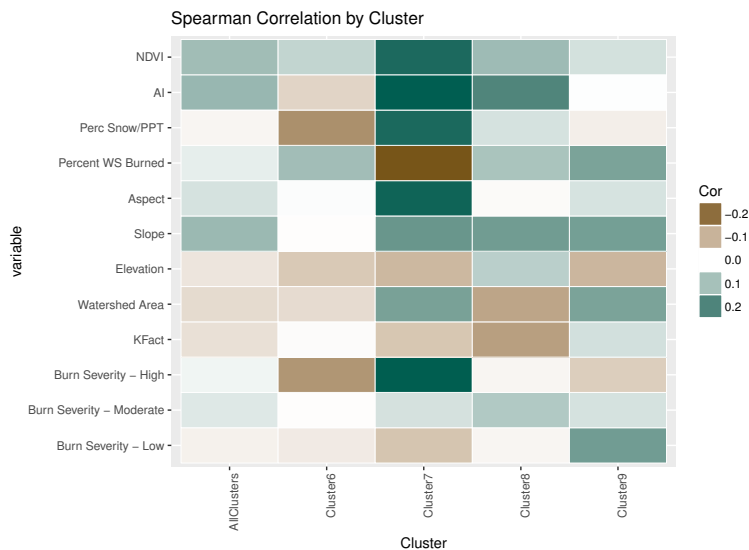
Figure 12. Heatmap of the averaged Spearman correlation coefficients of independent variables versus response variables, by cluster.

Correlation coefficients tend to be most significantly different within Cluster 6, where NDVI, AI, percent area burned, KFACT, high burn severity, and moderate burn severity show values contradicting those produced for Clusters 7-8, as well as for the fires as a whole. This is most likely indicative of a significant difference in response patterns for the region. Unfortunately, identifying significant trends is difficult given the relatively small dataset currently available.

5   Figure 13 demonstrates the correlation coefficients found across all fires. The largest absolute correlation value is 0.32 and only 20% of coefficients are greater than 0.10. However, as relative fire size is progressively limited to larger and larger values, correlation coefficients increase. NDVI, AI, percent watershed burned, slope, high burn severity, and moderate burn severity are dominantly positively correlated with flow response. Low burn severity, KFACT, and watershed area are dominantly negatively correlated with flow response. Elevation and %Snow/PPT display more varied correlations, but are generally negatively

10   correlated with flow response. From these results, we can surmise that as the NDVI, AI, percent area burned, slope, and moderate/high burn severity increase, flow response values will increase as well. Furthermore, as low burn severity, KFACT, and watershed area increase, flow response will decrease.

4.3.2   Regression

Figure 14 show the beta (coefficient) values produced by averaging the results of the linear and logistic regression models.

15   The resulting betas are highly variable and thus trends are difficult to interpret. To clarify results, Figure 15 is provided with logical values, where positive and negative betas are shown as values 1 and -1, respectively. Some trends are in agreement with those of the correlation results, such as moderate burn severity being positively correlated with response. Watershed area is also in agreement, showing negative correlation with response. All other independent variables that were dominant under
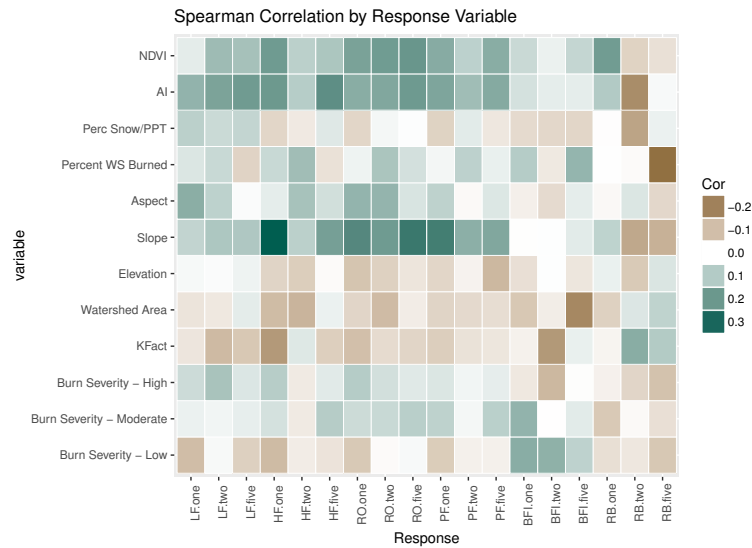
Figure 13. Heatmap of Spearman correlation coefficients of independent variables versus each response variable, for all watersheds. Response variables are abbreviated as LF (low flow), HF (high flow), RO (runoff ratio), PF (peak flow), BFI (base flow index), and RB (Richards-Baker). "One", "Two", and "Five" refer to the year of the response variable.

Spearman correlation are either too variable between clusters to accurately characterize, or are opposed to correlation results. For instance, NDVI and AI can be strongly positively or negatively correlated with response depending on cluster. High burn severity is shown to be negatively correlated with response across all clusters. Because the sample size of these clusters is so small (ranging from n=12 to 29), regression results may not be appropriate.

4.3.3 Random forest

Application of the random forest method provided little further insight into controlling watershed parameters. Applying the algorithm to the response values resulted in significant trees for only 1st year low flow, high flow, runoff ratio, and peak flow, as well as for 2nd year low flow. For the low flow response variables, area burned and aspect were the dominant controlling independent variables. For 1st year low flow, watersheds burned greater than 23.3% show the greatest response. Of those burned less than that threshold, some significant responses are found when burn areas have an aspect greater than 215 degrees. For 2nd year low flow, the largest responses are found in watersheds burned greater than 37%.

1st year high flow, runoff ratio, and peak flow are identified as being significantly affected by slope. Slopes of 7.0, 7.0, and 9.8 degrees divide response, respectively. Watersheds with greater than these slopes demonstrate much greater high flow, runoff ratio, and peak flow in the 1st year than those with gentler slopes.
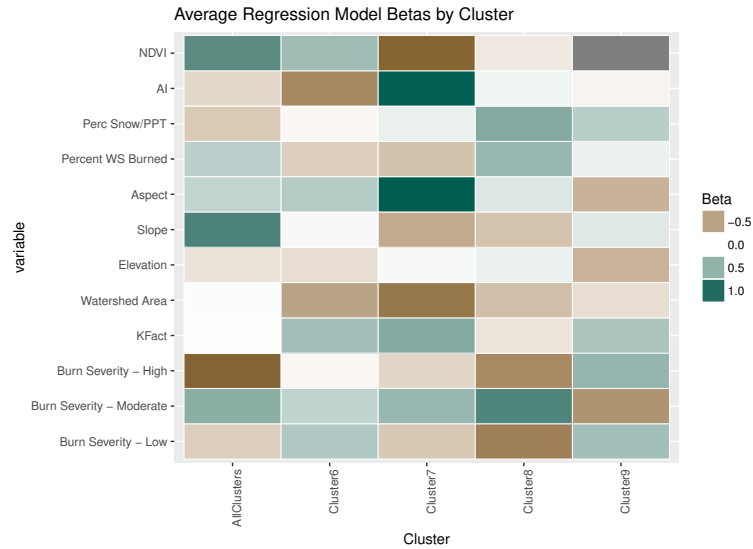
Figure 14. Heatmap of the averaged regression model beta values for each cluster.
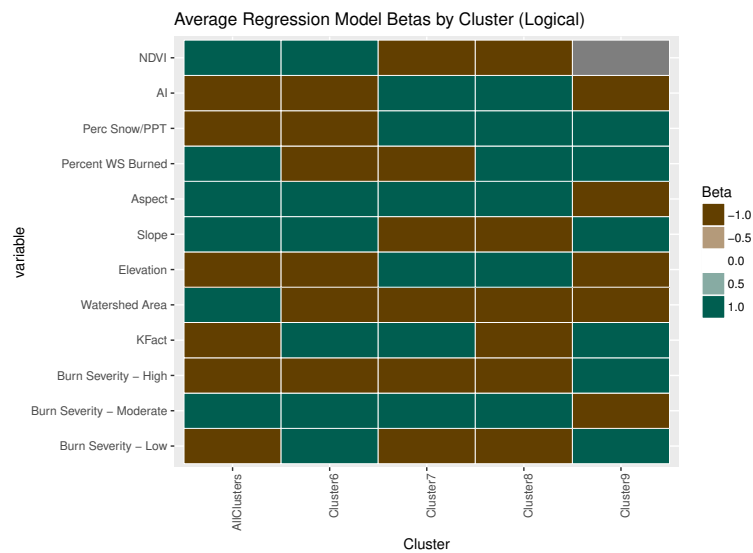
Figure 15. Heatmap of logical values of the averaged regression model beta values for each cluster shown in Figure 14.

4.3.4 Discussion of Geophysical Parameters

Through Spearman correlation, the independent variables NDVI, AI, percent area burned, slope, BS*H, and BS*M are positively correlated with post-fire flow response. BS*U, KFACT, and watershed area are negatively correlated with response. The results of several regression models are less clear, with inconstant relationships across all fires and clusters. Generally,

they show that only BS*M is dominantly positively correlated with response and that watershed area and, somehow BS*H are negatively correlated with response. Random forest analysis shows that significant relationships can be found for the LF.one, LF.two, HF.one, RO.one, and PF.one response variables. These relationships are dominated by dependence on either percent burn area or by slope.

5   Overall, results of geophysical parameter characterization are somewhat inconsistent, likely due to the sample size of this study. Though it is one of the largest to date, there are still too few fire events relative to the number of geophysical parameters to produce consistent results. What can be gleaned from the various methods used in this section is that slope is frequently a strong predictor of response. This is a reasonable assumption considering that steeper slopes lead to less time available for soil absorption, thus increasing the volume of water contributed to streamflow. Support for this argument is found in the Spearman
10 correlation coefficient analysis in Figures 12 and 13, where slope is shown to be strongly correlated with LF, HF, PF, and RO responses, as well as in the random forest analysis where slope is one of the few independent variables to be identified as significant. Determining the influence of independent variables on response at the cluster level seems, with this sample size, unreasonable. There is too much variance in flow regimes to complete a trend analysis with groupings of the size produced in this study. However, over the next decade the sample size of this study should be able to be increased significantly and provide
15 a more robust dataset for analysis.

5   Conclusions

Post-fire changes in streamflow are found to be highly variable across regions of the western U.S. and some trends can be difficult to discern. In general, flow response for the study watersheds was found to be greatest in both magnitude and variability within the 1st year following a fire and shown to decrease over a five year period. However, upon examination of response by
20 cluster we find that these general trends are dominated by the high-magnitude responses of watersheds from Cluster 8. While watersheds from Clusters 6 and 9 do not show identifiable trends, Cluster 7 shows decreased responses in the 1st year following fires and positive, increasing responses in the 2nd and five year means, indicating that Cluster 7 watersheds yield a more delayed flow response. The results from Cluster 8, a dominantly chaparral environment, agree with other studies both within the same region (Coombs and Melack, 2013; Kinoshita and Hogue, 2011 and 2015; Loáiciga et al., 2001) and in chaparral
25 environments outside the United States (Hessling, 1999; Lavabre et al., 1993; Lindley et al., 1988; Scott, 1993). As mentioned in the introduction, some studies find little to no change in streamflow post-fire (Aronica et al., 2002; Bart and Hope, 2010; Britton, 1991; Townsend and Douglas, 2000). This study similarly identifies several regions (Clusters 6 and 9) that also do not show distinguishable trends.

Identification of controlling watershed parameters on response yielded somewhat weak results. Various methods showed
30 sometimes contrary results, or none at all. Spearman correlation indicated that watershed slope, NDVI, AI, and %Snow/PPT are positively correlated with flow response. Low burn severity, Kfact, and watershed area were shown to be negatively correlated with response. These correlations are largely in agreement with the positions asserted by Moody et al. (2013), Biggio and Cannon (2001), and Neary et al. (2005).

Regression models showed that only moderate burn severity and watershed area are consistently positively and negatively correlated, respectively, with flow response. Random forest models indicated that percent area burned and slope are the only significant factors, and only for 1st year response metrics. The observed changes in streamflow following wildfire identified in this study have wide-ranging implications on regional water budgets, downstream flood response, long-term water yield, and post-fire watershed modeling. Improved streamflow predictions allow water resource managers in water-limited regions to anticipate surplus volume in their budgeting forecast calculations and also help flood forecasters to identify areas at greater risk for damage and infrastructure overload. Identification of the influence of watershed geophysical parameters on post-fire streamflow should also enable improved calibration of regional models for burned watersheds.

Acknowledgements. This work was partially supported by a USGS internship through the Colorado Water Science Center.

References

Aronica, G., Candela, A., and Santoro, M. (2002). Changes in the hydrological response of two Sicilian basins affected by fire. (IAHS Press), pp. 163–169.

Baker, D.B., Richards, R.P., Loftus, T.T., and Kramer, J.W. (2004). A New Flashiness Index: Characteristics and Applications to Midwestern Rivers and Streams1. JAWRA Journal of the American Water Resources Association 40, 503–522.

Barbosa, P.M., Stroppiana, D., Gregoire, J.M., and Pereira, J.M.C. (1999). An assessment of vegetation fire in Africa (1981-1991): Burned areas, burned biomass, and atmospheric emissions. Glob. Biogeochem. Cycle 13, 933–950.

Bart, R., and Hope, A. (2010). Streamflow response to fire in large catchments of a Mediterranean-climate region using paired-catchment experiments. Journal of Hydrology 388, 370–378.

Benavides-Solorio, J., and MacDonald, L.H. (2001). Post-fire runoff and erosion from simulated rainfall on small plots, Colorado Front Range. Hydrol. Process. 15, 2931–2952.

Biggio, E.R., and Cannon, S.H. (2001). Compilation of post-wildfire runoff data from the Western United States (U.S. Geological Survey).

Bond, N. (2015). hydrostats: Hydrologic Indices for Daily Time Series Data.

Britton, D.L. (1991). Fire and the chemistry of a South African mountain stream. Hydrobiologia 218, 177–192.

Burke, M.P., Hogue, T.S., Ferreira, M., Mendez, C.B., Navarro, B., Lopez, S., Jay, J.A. (2010). The effect of wildfire on soil mercury concentrations in southern California watersheds. Water, Air, Soil Pollution 212, 369-385.

Burke, M.P., Hogue, T.S., Kinoshita, A., Barco, J., Wessel, C., Stein, E. (2013). Pre- and post-fire pollutant loads in an urban watershed in southern California. Environmental Monitoring and Assessment 185, 10131-10145.

Cannon, S.H., Kirkham, R.M., and Parise, M. (2001). Wildfire-related debris-flow initiation processes, Storm King Mountain, Colorado. Geomorphology 39, 18.

Carlson, T.N., and Ripley, D.A. (1997). On the relation between NDVI, fractional vegetation cover, and leaf area index. Remote Sensing of Environment 62, 241–252.

Coombs, J.S., and Melack, J.M. (2013). Initial impacts of a wildfire on hydrology and suspended sediment and nutrient export in California chaparral watersheds. Hydrol. Process. 27, 3842–3851.

DeBano, L.F. (2000). The role of fire and soil heating on water repellency in wildland environments: a review. J. Hydrol. 231, 195–206.

Eidenshink, J., Schwind, B., Brewerm K., Zhu, Z., Quayle, B., Howard, S. (2007). A project for monitoring trends in burn severity. Fire Ecology Special Issue 3.

Emelko, M.B., Silins, U., Bladon, K.D., and Stone, M. (2011). Implications of land disturbance on drinking water treatability in a changing climate: Demonstrating the need for "source water supply and protection" strategies. Water Research 45, 461–472.

Emmerich, W.E., and Cox, J.R. (1994). Changes in Surface Runoff and Sediment Production after Repeated Rangeland Burns. Soil Science Society of America Journal 58, 199.

Falcone, J. (2011). GAGES-II: Geospatial Attributes of Gages for Evaluating Streamflow (Reston, Virginia: U.S. Geological Survey).

Fraley, C., Raftery, A.E., Murphy, T.B., and Scrucca, L. (2012). mclust Version 4 for R: Normal Mixture Modeling for Model-Based Clustering, Classification, and Density Estimation (Department of Statistics, University of Washington).

Goldman, S.J., Jackson, K., and Bursztynsky, T.A. (1986). Erosion and sediment control handbook (McGraw-Hill).

Google, Inc. Google Earth Engine. Accessed 2015.

Hessling, M. (1999). Hydrological modelling and a pair basin study of mediterranean catchments. Physics and Chemistry of the Earth, Part B: Hydrology, Oceans and Atmosphere 24, 59–63.

Hester, J.W., Thurow, T.L., and Charles A. Taylor, J. (1997). Hydrologic Characteristics of Vegetation Types as Affected by Prescribed Burning. Journal of Range Management 50, 199–204.

Homer, C., Huang, C., Wylie, B., and Coan, M. (2004). Development of a 2001 National Landcover Database for the United States. Photogrammetric Engineering and Remote Sensing 70, 829–840.

Hothorn, T, Hornik, K., Zeileis, A. (2006). Unbiased Recursive Partitioning: A Conditional Inference Framework. Journal of Computational and Graphical Statistics, 15(3), 651–674.

Kinoshita, A.M., and Hogue, T.S. (2011Spatial and temporal controls on post-fire hydrologic recover in southern California watersheds. Catena 87, 240-252.

Kinoshita, A.M., and Hogue, T.S. (2015). Increased dry season water yield in burned watersheds in Southern California. Environ. Res. Lett. 10, 014003.

Ladson, A.R., Brown, R., Neal, B., Nathan, R. (2013). A standard approach to baseflow separation using the Lyne and Hollick filter. Australian Journal of Water Resources 17, 24-34.

Lavabre, J., Torres, D.S., and Cernesson, F. (1993). Changes in the hydrological response of a small Mediterranean basin a year after a wildfire. Journal of Hydrology 142, 273–299.

Lee, R.J., and Chow, T.E. (2015). Post-wildfire assessment of vegetation regeneration in Bastrop, Texas, using Landsat imagery. GISci. Remote Sens. 52, 609–626.

Lindley, A.J., Bosch, J.M., and van Wyk, D.B. (1988). Changes in water yield after fire in fynbos catchments. Water SA 14, 7–12.

Littell, J.S., McKenzie, D., Peterson, D.L., and Westerling, A.L. (2009). Climate and wildfire area burned in western U.S. ecoprovinces, 1916–2003. Ecological Applications 19, 1003–1021.

Loaiciga, H.A., Pedreros, D., and Roberts, D. (2001). Wildfire-streamflow interactions in a chaparral watershed. Advances in Environmental Research 5, 295–305.

MacQueen, J. (1967). Some methods for classification and analysis of multivariate observations. (The Regents of the University of California).

McManamay, R.A., Bevelhimer, M.S., and Kao, S.-C. (2014). Updating the US hydrologic classification: an approach to clustering and stratifying ecohydrologic data. Ecohydrol. 7, 903–926.

Meyer, G.A., Pierce, J.L., Wood, S.H., and Jull, A.J.T. (2001). Fire, storms, and erosional events in the Idaho batholith. Hydrol. Process. 15, 3025–3038.

Moody, J.A., and Martin, D.A. (2001). Initial hydrologic and geomorphic response following a wildfire in the Colorado Front Range. Earth Surface Processes and Landforms 26, 1049–1070.

Moody, J.A., Shakesby, R.A., Robichaud, P.R., Cannon, S.H., and Martin, D.A. (2013). Current research issues related to post-wildfire runoff and erosion processes. Earth-Science Reviews 122, 10–37.

Moritz, M.A., Moody, T.J., Krawchuk, M.A., Hughes, M., and Hall, A. (2010). Spatial variation in extreme winds predicts large wildfire locations in chaparral ecosystems. Geophys. Res. Lett. 37, L04801.

National Wildfire Coordinating Group. Glossary of Wildland Fire Terms, accessed 2016.

Neary, D.G. (2003). Post-wildfire watershed flood responses.

Neary, D.G., Ryan, K.C., and DeBano, L.F.; (2005). Wildland fire in ecosystems: effects of fire on soils and water.

Owens, P.N., Giles, T.R., Petticrew, E.L., Leggat, M.S., Moore, R.D., and Eaton, B.C. (2013). Muted responses of streamflow and suspended sediment flux in a wildfire-affected watershed. Geomorphology 202, 128–139.

Pausas, J.G., Llovet, J., Rodrigo, A., and Vallejo, R. (2008). Are wildfires a disaster in the Mediterranean basin? – A review. International Journal of Wildland Fires 17(6), 713–723.

5   Pierson, F.B., Moffet, C.A., Williams, C.J., Hardegree, S.P., and Clark, P.E. (2009). Prescribed-fire effects on rill and interrill runoff and erosion in a mountainous sagebrush landscape. Earth Surface Processes and Landforms 34, 193-203.

Poff, N. (1996). A hydrogeography of unregulated streams in the United States and an examination of scale-dependence in some hydrological descriptors. Freshwater Biology 36, 71–79.

PRISM Climate Group (2004). Oregon State University, http://prism.oregonstate.edu.

10   Santos, R.M.B., Sanches Fernandes, L.F., Pereira, M.G., Cortes, R.M.V., and Pacheco, F.A.L. (2015). Water resources planning for a river basin with recurrent wildfires. Science of The Total Environment 526, 1–13.

Schwartz, G.E., and Alexander, R.B. (1995). Soils data for the Conterminous United States Derived from the NRCS State Soil Geographic (STATSGO) Data Base.

Schwarz, G. (1978). Estimating the Dimension of a Model. Ann. Statist. 6, 461–464.

15   Scott, D.F. (1993). The hydrological effects of fire in South African mountain catchments. J Hydrol. Journal of Hydrology 150, 409–432.

Shakesby, R.A., and Doerr, S.H. (2006). Wildfire as a hydrological and geomorphological agent. Earth-Sci. Rev. 74, 269–307.

Smith, H.G., Sheridan, G.J., Lane, P.N.J., Nyman, P., and Haydon, S. (2011). Wildfire effects on water quality in forest catchments: A review with implications for water supply. Journal of Hydrology 396, 170–192.

Stein, E.D., Brown, J.S., Hogue, T.S., Burke, M.P., and Kinoshita, A. (2012). Stormwater contaminant loading following southern California
20   wildfires. Environ. Toxicol. Chem. 31, 2625–2638.

Townsend, S.A., and Douglas, M.M. (2000). The effect of three fire regimes on stream water quality, water yield and export coefficients in a tropical savanna (northern Australia). Journal of Hydrology 229, 118–137.

U.S. Geological Survey (2014). National Water Information System—NWISWeb: accessed on various dates in 2014 at http://waterdata.usgs.gov.

25   Watson, F., Vertessy, R., McMahon, T., Rhodes, B., and Watson, I. (2001). Improved methods to assess water yield changes from paired-catchment studies: application to the Maroondah catchments. Forest Ecology and Management 143, 189–204.

Westerling, A.L., Hidalgo, H.G., Cayan, D.R., and Swetnam, T.W. (2006). Warming and earlier spring increase western US forest wildfire activity. Science 313, 940–943.

Westerling, A.L. (2016). Increasing western US forest wildfire activity: sensitivity to changes in the timing of spring. Philosophical Transac-
30   tions of the Royal Society B (371).

Wilkinson, S.N., Wallbrink, P.J., Hancock, G.J., Blake, W.H., Shakesby, R.A., and Doerr, S.H. (2009). Fallout radionuclide tracers identify a switch in sediment sources and transport-limited sediment yield following wildfire in a eucalypt forest. Geomorphology 110, 140–151.

Whitlock, C. (2004). Land management: Forests, fires and climate. Nature 432, 28–29.

Woodcock, C.E., Allen, R., Anderson, M., Belward, A., Bindschadler, R., Cohen, W., Gao, F., Goward, S.N., Helder, D., Helmer, E., Nemani,
35   R., Oreopoulos, L., Schott, J., Thenkabail, P.S., Vermote, E.F., Vogelmann, J., Wulder, M.A., Wynne, R. (2008). Free access to Landsat imagery. Science 320.